Multi-Agent Reinforcement Learning for Joint Police Patrol and Dispatch

Matthew Repasky, He Wang, and Yao Xie

H. Milton Stewart School of Industrial and Systems Engineering, Georgia Institute of Technology

Abstract

Police patrol units need to split their time between performing preventive patrol and being dispatched to serve emergency incidents. In the existing literature, patrol and dispatch decisions are often studied separately. We consider joint optimization of these two decisions to improve police operations efficiency and reduce response time to emergency calls. Methodology/results: We propose a novel method for jointly optimizing multi-agent patrol and dispatch to learn policies yielding rapid response times. Our method treats each patroller as an independent Q-learner (agent) with a shared deep Q-network that represents the state-action values. The dispatching decisions are chosen using mixed-integer programming and value function approximation from combinatorial action spaces. We demonstrate that this heterogeneous multi-agent reinforcement learning approach is capable of learning joint policies that outperform those optimized for patrol or dispatch alone. $Managerial\ Implications$: Policies jointly optimized for patrol and dispatch can lead to more effective service while targeting demonstrably flexible objectives, such as those encouraging efficiency and equity in response.

1 Introduction

The timeliness of police response to emergency calls plays a critical role in maintaining public safety and preventing crimes. However, recent data showed that police response times in major U.S. cities are getting longer, partly due to staffing shortages (Kaste 2023). In this paper, we study how to improve police patrol operations and reduce emergency call response times by multi-agent reinforcement learning, where each patrol unit (e.g., a police patrol car) is treated as an agent.

Coordinating the patrol of multiple agents in a shared environment has been a task of interest in operations research and machine learning for many years. Approaches ranging from extensions of the traveling salesman problem (Chevaleyre 2004) to deep reinforcement learning (RL) for multi-agent robot patrol (Jana et al. 2022) have been applied. Many challenges are associated with multi-agent patrol, including large action spaces that grow exponentially with the number of patrollers, coordination/cooperation of agents, and state representation. Some prior works evaluate patrol policies using criteria that capture "coverage," such that all locations are visited frequently (Almeida et al. 2004). Instead, in this work, we evaluate patrol policies with respect to a separate but related task: multi-agent dispatch.

The police dispatching problem has traditionally been considered using multi-server priority queues (Green 1984). The task of a dispatcher is to select a patroller to dispatch to the scene of an incident. Recent efforts have considered the effects of dispatch policies given positioning and/or routing of patrollers in some space (e.g., a grid or a graph) (Guedes et al. 2015, Dunnett et al. 2019). Oftentimes, the response times to incidents must meet some key performance indicators (Stanford et al. 2014), which has also been considered in the context of dispatch (Zhang et al. 2016).

The positioning of patrollers is key to effective dispatch, yet most dispatch works consider heuristic patrol policies. Early works considering multi-agent patrol (without dispatch) coordinated individual agent patrol decisions using heuristics such as neighboring node idleness (Machado et al. 2003). Others considered extensions of the single-patroller traveling salesman problem to multiple agents (Chevaleyre 2004). Multi-agent reinforcement learning (MARL) for multi-agent patrolling has also been considered for many years

^{*}Email: mwrepasky@gatech.edu

(Santana et al. 2004); e.g., node idleness can be minimized by independent learners with cooperative rewards. Early RL approaches considered individual patrollers who only had information about their local environment but could communicate with others about intended actions. More recently, multi-agent patrol policies have been learned using Bayesian learning (Portugal et al. 2013) and deep RL (Jana et al. 2022). A common theme is distributed policy optimization with varying degrees of communication between agents, where the goal is to optimize with respect to idleness or frequency of visits to each location.

In addition to a growing need for efficient police operations in light of staffing shortages and limited resources in recent years (The Associated Press 2023, Charalambous 2023, Hermann 2023), fairness and equity in operations such as patrol and dispatch is an area of increased interest, and the benefits of such considerations are plentiful. For instance, Dickson et al. (2022) shows that police officers who are perceived to be fair are more likely to observe respect and legitimacy with their community. Moreover, opinions within the US justice system echo the sentiment that fairness in law enforcement is crucial for public cooperation and support (Waldschmidt 2018). The importance of this issue is highlighted by many police departments across the US, often posting statements and procedures regarding fairness in their operations (Parker Police Department 2024, Notre Dame Police Department 2024, Walker 2023). Algorithmic considerations of fairness in police operations typically focus on providing equity in service to multiple groups (Wheeler 2020, Liberatore et al. 2023).

To our knowledge, ours is the first work to optimize policies for patrol and dispatch jointly. Our contributions are as follows.

• Jointly-optimized policies for patrol and dispatch: Prior dispatch optimization strategies typically assume heuristic patrol policies. Similarly, prior multi-agent patrolling works do not jointly optimize separate decision tasks such as dispatch. We outline a procedure to optimize policies for patrol and dispatch jointly, outperforming benchmark policies optimized for patrol or dispatch alone in addition to heuristic policies such as priority queue dispatch. We demonstrate that the superior performance of our method is robust to a range of simulated environments of varying sizes and dynamics and with different objectives.

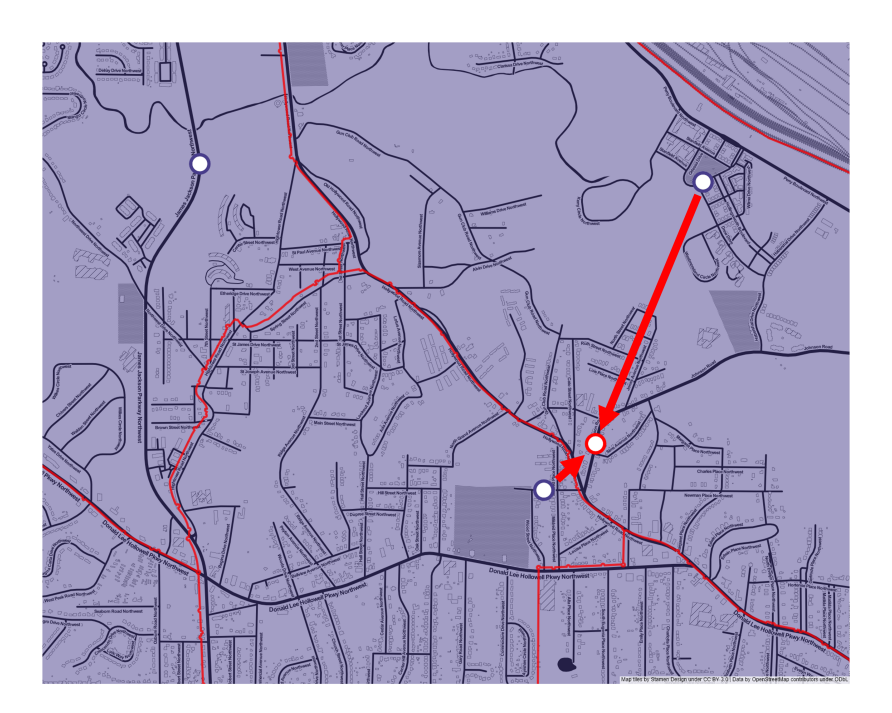


Figure 1: The joint task of patrol and dispatch involves decisions such as that demonstrated above. It is unclear whether it is best to move one patroller across beat boundaries to manage an incident, leaving its beat un-managed, or to require the patroller responsible for that beat to travel a long distance to the scene.

- Novel optimization approach: We use distributed MARL with parameter sharing to exploit similarities between patrollers while jointly optimizing a dispatcher agent whose action space has combinatorial cardinality. We extend recent works in combinatorial RL to systems with stochastic transitions. We incorporate them into our MARL framework via a coordinate-descent-style alternating optimization of patrol and dispatch policies.
- Fairness and real service systems: We demonstrate that our approach is flexible to various reward definitions, such as those that encourage equitable policies. Policies that explicitly encode equity in the reward definition yield more balanced responses to groups of different sizes. We also apply our approach to scenarios based on real calls-for-service data.

1.1 Related works

RL is a machine learning approach for training an agent to make sequential decisions in a stochastic environment (Sutton and Barto 2018, Bertsekas 2019). Deep RL uses neural networks, such as deep Q networks (DQNs), to learn policies (Mnih et al. 2015). Making decisions for multiple agents is a central issue in MARL, as the number of possible actions is exponential in the number of agents. Independent Q-learning (IQL) (Tan 1993) addresses this by decomposing the problem into multiple single-agent RL problems. Each agent operates in the same environment, but there are no guarantees regarding cooperation and interference; nonetheless, the naive extension of DQNs to the IQL framework has been successful in some cases (Gupta et al. 2017, Tampuu et al. 2017). To address cooperation and efficiency in distributed MARL, parameter sharing in deep RL has been employed (Gupta et al. 2017, Chu and Ye 2017, Terry et al. 2020, Christianos et al. 2021, Chen et al. 2021, Yu et al. 2022). Greater degrees of parameter sharing are often most effective between agents with similar value spaces and reward functions.

Multi-agent patrol has been investigated from the perspective of operations research (Chevaleyre 2004), Bayesian learning (Portugal et al. 2013), and (deep) MARL (Santana et al. 2004, Jana et al. 2022). Many of these works pose the problem as a discrete-time, discrete-location graph traversal (Almeida et al. 2004, Portugal and Rocha 2010, Portugal et al. 2013). Past works recognize the inherent complexity of making a centralized decision to patrol many agents and decompose the problem via distributed optimization (Santana et al. 2004, Farinelli et al. 2017). Similarly, our approach to learning multi-agent patrol policies is distributed while addressing issues arising from the decentralized decision-making for multiple cooperative agents. Additionally, we consider this problem in conjunction with a separate but connected dispatch task, which is not thoroughly addressed in prior work.

Dispatch of multiple patrollers and resources is typically considered from the queueing or ranking systems perspective. Zhang et al. (2016) investigate such a setting using static and dynamic priority queues, connecting to the queuing literature in developing dispatch policies and indicating the static queues yield better performance. For instance, Guedes et al. (2015) construct a ranking system based on quantitative incident characteristics, such as arrival time, priority, and distance to the nearest patroller. Similarly, Dunnett et al. (2019) formulates the dispatch decision process by constructing multiple queues, considering incident categories and severity, amongst other factors such as routing of units. Crucially, prior works regarding dispatch in service systems neglect to optimize multi-agent patrol policies, typically assuming basic heuristics.

A typical notion of fairness in machine learning applications suggests that the outcome of an algorithm should be independent of the group to which it is applied (Barocas et al. 2017). In the context of service operations such as police patrol and dispatch, such groups can be defined by socioeconomic or racial status. For example, fairness has been studied in the police districting problem to improve efficiency while mitigating racial disparity in defining patrol districts (Liberatore et al. 2022, 2023). Parallel works have worked to alleviate disproportionate minority contact that can arise due to hot spot policing (Wheeler 2020). Such works find that simply neglecting to take sensitive features (e.g., race or location) into account is ineffective at achieving fairnesss (Eckhouse et al. 2019). Therefore, these attributes are taken into account in decision-making problems to encode fairness explicitly, often leading to a minimal tradeoff in efficiency.

2 Background

This section provides the necessary background information regarding reinforcement learning (RL) and multi-agent reinforcement learning (MARL) as applied to service systems such as police patrol and dispatch.

2.1 Single-Agent Reinforcement Learning

An infinite-horizon discounted Markov Decision Process (MDP) can be represented by a tuple $\langle \mathcal{S}, \mathcal{A}, \mathbb{P}, R, \gamma \rangle$ with state space \mathcal{S} , action space \mathcal{A} , transition dynamics $\mathbb{P}: \mathcal{S} \times \mathcal{A} \to \Delta(\mathcal{S})$, reward function $R: \mathcal{S} \times \mathcal{A} \times \mathcal{S} \to \mathbb{R}$, and discount $\gamma \in [0, 1)$. The goal of RL (Bertsekas 2019) is to learn a policy $\pi: \mathcal{S} \to \mathcal{A}$ maximizing cumulative discounted reward, captured by the value function $V^{\pi}: \mathcal{S} \to \mathbb{R}$:

$$V^{\pi}(s_0) = \mathbb{E}\left[\sum_{t\geq 0} \gamma^t R\left(s_t, \pi(s_t), s_{t+1}\right)\right],$$

beginning in state s_0 and following $a_t \sim \pi(s_t)$, where s_t is the state in period t. A policy that maximizes the value function $V^{\pi}(s_0)$ above is called an optimal policy and is denoted by π^{\star} . Let V^{\star} be the optimal value function.

It is often more convenient to consider the state-action value (Q-value) in RL:

$$Q^{\pi}(s_0, a_0) = \mathbb{E}\left[R(s_0, a_0, s_1) + \sum_{t \ge 1} \gamma^t R(s_t, \pi(s_t), s_{t+1})\right].$$

The state value $V^{\pi}(s)$ and the state-action value $Q^{\pi}(s, a)$ are connected by $V^{\pi}(s) = Q^{\pi}(s, \pi(s))$. Let Q^{\star} be the optimal Q-value. The optimal policy π^{\star} takes greedy actions with respect to Q^{\star} : $\pi^{\star}(s) = \arg\max_{a \in \mathcal{A}} Q^{\star}(s, a)$. Since $V^{\star} = \max_{a} Q^{\star}(s, a)$, the Bellman optimality equation reveals:

$$Q^{\star}(s, a) = \mathbb{E}\left[R(s, a, s') + \gamma V^{\star}(s')\right].$$

2.1.1 Deep Q-Learning.

Q-learning is a model-free RL technique to learn the optimal state-action value function by exploiting the Bellman optimality condition (Watkins 1989). Q^{π} , approximated by a function parameterized by θ , can be learned given transitions $(s_t, a_t, s_{t+1}, r_t) \in \mathcal{D}$, where $r_t := R(s_t, a_t, s_{t+1})$ and \mathcal{D} sampled from the MDP. Parameter θ can then be learned by minimizing the least-squares value iteration (LSVI) objective (Bradtke and Barto 1996):

$$\hat{\theta} = \underset{\theta}{\operatorname{argmin}} \left(\sum_{(s_t, a_t, s_{t+1}, r_t) \in \mathcal{D}_{\ell} \subset \mathcal{D}} \left(r_t + \gamma \max_{a} Q^{\tilde{\theta}}(s_{t+1}, a) - Q^{\theta}(s_t, a_t) \right)^2 \right),$$

A deep Q-network (DQN) (Mnih et al. 2015) $Q^{\theta}: \mathbb{R}^d \to \mathbb{R}^{|\mathcal{A}|}$ is often used as the approximator, taking $s \in \mathcal{S} \subset \mathbb{R}^d$ and outputting $Q^{\theta}(s, a)$ values for each action. Target networks parameterized by $\tilde{\theta}$, a copy of θ cloned every L updates, are often used to stabilize optimization.

2.1.2 Value Function Approximation.

One might instead want to approximate $V^{\pi}(s)$ given policy π . Assume tuples $(s_t, \tilde{r}_t) \in \mathcal{E}$ are observed, where $\tilde{r}_t := \sum_{t' \geq t} \gamma^{t'-t} R(s_{t'}, \pi(s_{t'}), s_{t'+1})$ is the discounted sum of reward following state s_t under policy π . Value $V^{\pi}(s)$ can be approximated by a function V^{ϕ} parameterized by ϕ to minimize the following objective:

$$\hat{\phi} = \underset{\phi}{\operatorname{argmin}} \left(\sum_{(s_t, \tilde{r}_t) \in \mathcal{E}} \left(V^{\phi}(s_t) - \tilde{r}_t \right)^2 \right).$$

2.1.3 Reinforcement Learning with Combinatorial Action Space

If $|\mathcal{A}|$ is too large to enumerate (e.g., selection amongst combinatorially-many sets of pairings), Q-learning is not applicable since it must enumerate all action values. Let $x_{ij} = 1$ if i is paired to j, with $x_{ij} = 0$ otherwise. Define d_{ij} the reward for this pairing. Since the optimal action maximizes the current reward plus the next state value (Delarue et al. 2020):

$$\pi(s) = \underset{\{x_{ij}\}}{\operatorname{argmax}} \sum_{i} \sum_{j} d_{ij} x_{ij} + V^{\pi}(s'),$$

subject to problem-specific constraints. If s' can be computed given the action and V^{π} is approximated as in Section 2.1.2, actions are selected by solving a mixed-integer program (MIP).

2.2 Multi-Agent Reinforcement Learning

Given agents $i=1,\ldots,N$, centralized MARL formulates decision-making as an MDP (Gupta et al. 2017); one agent learns a policy π mapping states to a joint action in $\mathcal{A}_1 \times \cdots \times \mathcal{A}_N$. IQL addresses the exponential growth of this joint action space by learning N functions Q^{θ_i} (Tan 1993). Agent i operates within the single-agent MDP represented by the tuple $\langle \mathcal{S}, \mathcal{A}_i, \mathbb{P}_i, R_i, \gamma_i \rangle$. When the agents are similar, parameter sharing can accelerate learning, acting as an intermediate between centralized MARL and IQL (Gupta et al. 2017).

MARL can also be described using a Markov game (MG) (Littman 1994) formulation, defined by a tuple $\langle N, \mathcal{S}, \{\mathcal{S}_i\}_{i=1}^N, \{\mathcal{A}_i\}_{i=1}^N, \mathbb{P}, \{R_i\}_{i=1}^N, \gamma \rangle$, including a universal state space \mathcal{S} , "perspectives" $\{\mathcal{S}_i\}_{i=1}^N$, joint action space $\mathcal{A} = \mathcal{A}_1 \times \cdots \times \mathcal{A}_N$, transition dynamics $\mathbb{P} : \mathcal{S} \times \mathcal{A} \to \Delta(\mathcal{S})$, reward functions $R_i : \mathcal{S} \times \mathcal{A} \times \mathcal{S} \to \mathbb{R}$, and discount γ . The goal is to maximize the expected discounted sum of future reward for each agent $\tilde{V}_i^{\pi}(s_0) = \mathbb{E}\left[\sum_{t\geq 0} \gamma^t R_i\left(s_t, \pi(s_t), s_{t+1}\right)\right]$, where $s_0 \in \mathcal{S}$ is an initial universal state and $\pi = (\pi_1, \dots, \pi_N)$ is a joint policy. Similarly:

$$\tilde{Q}_{i}^{\pi}(s_{0}, a_{0}) = \mathbb{E}\left[R_{i}(s_{0}, a_{0}, s_{1}) + \sum_{t \geq 1} \gamma^{t} R_{i}(s_{t}, \pi(s_{t}), s_{t+1})\right]. \tag{1}$$

Each \tilde{V}_i^{π} is meant to be maximized with respect to all other policies, such that

$$\pi_i = \operatorname*{argmax}_{\pi_i'} \tilde{V}_i^{\pi'} \text{ where } \pi' = (\pi_1, \dots, \pi_i', \dots, \pi_N).$$

IQL can be employed to optimize each π_i . Moreover, if $\{S_i\}_{i=1}^N$, $\{A_i\}_{i=1}^N$, and $\{R_i\}_{i=1}^N$ are similar among all agents, parameter sharing can be employed to learn the policies.

2.3 Police Operations

Police jurisdictions are typically hierarchically divided. For example, the Atlanta Police Department (APD) divides the city of Atlanta into six *zones*, each of which is divided into *beats* (Atlanta Police Department 2023). One patroller is usually assigned to each beat. When calls-for-service arrive at the dispatcher, an officer in the same zone as the incident is dispatched to the scene; a patroller can be dispatched to a call outside their assigned beat. This joint problem of beat-based patrol and dispatch is further discussed and formalized in Section 3.

3 Problem Formulation

Consider patrollers i = 1, ..., N making decisions in time t = 1, 2, ... Joint patrol and dispatch is formalized as an MDP with a central agent and then is decomposed into an MG of N + 1 agents.

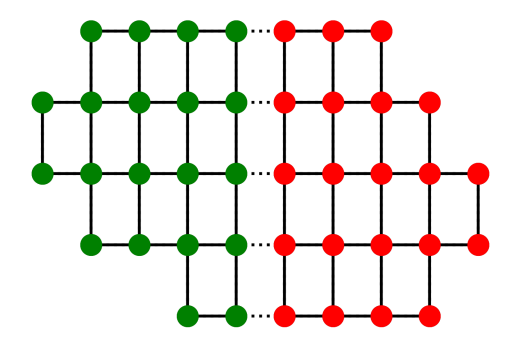


Figure 2: Example of a graph with two beats indicated by color. The dotted edges indicate that patrollers can travel between beats only when responding to calls.

3.1 The Patrol Problem

Patrollers navigate a connected, undirected graph G = (V, E) (Almeida et al. 2004) with nodes/locations V connected by edges E which are traversed in a single iteration; each $v \in V$ is connected to itself. Each patroller i is assigned to a node subset (beat) V_i , an example is visualized in Figure 2. The patrol problem involves travel decisions for each patroller. For patrollers not busy responding to incidents (Sections 3.2 and 3.3), a patrol policy directs each patroller to a neighboring node in V_i .

3.2 The Dispatch Problem

Incidents of categories $k=1,\ldots,K$ arrive with rates λ_k following distributions $q_k(v)$ supported on V, requiring $t_{\text{scene}} \sim \text{Exp}(\beta_k)$ on-scene time to manage. The dispatch problem involves matching free patrollers (not currently dispatched) to idle incidents (not yet been assigned). A dispatch policy selects among all possible groups of pairings, including leaving incidents idle or patrollers free. A dispatched patroller travels along the shortest path towards the incident, whose number of edges is equivalent to the travel time t_{travel} in iterations. If a patroller arrives at iteration t, it is finished managing the incident starting at iteration $t + t_{\text{scene}}$.

3.3 Joint Patrol & Dispatch

The service time for patroller i to manage incident j is $t_{\text{service}}(i,j) = t_{\text{idle}}(j) + t_{\text{travel}}(i,j) + t_{\text{scene}}(j)$, where $t_{\text{idle}}(j)$ is the time spent in the queue before dispatch. When patroller i is dispatched, it must travel toward the incident or remain at the scene. When outside its beat, it must return once free. Define the response time, reflecting the time incident j waited before patroller i arrived:

$$t_{\text{response}}(i,j) = t_{\text{idle}}(j) + t_{\text{travel}}(i,j).$$
 (2)

Joint patrol and dispatch can be formulated as an MDP to learn joint policy π .

3.3.1 Joint State Space.

Given patroller positions $v_1, \ldots, v_N \in V$ and busy statuses $u_1, \ldots, u_N \in \mathbb{N}$ (travel and on-scene time), define $\mathbf{v} := [(v_1, u_1), \ldots, (v_N, u_N)]$. At dispatch, patrollers observe the random on-scene service time. Given locations of M idle incidents $w_1, \ldots, w_M \in V$ and idle times $p_1, \ldots, p_M \in \mathbb{N}$, define $\mathbf{w} := [(w_1, p_1), \ldots, (w_M, p_M)]$. The queue has a fixed idle-incident capacity M; when full and a new incident arrives, the longest-waiting incident is replaced. The joint state space is $\mathcal{S} = \{s = [\mathbf{v} \oplus \mathbf{w}]^T\}$, where \oplus refers to vector concatenation.

3.3.2 Joint Action Space.

For a free patroller, patrol action set $\mathcal{A}_i^{(\text{patrol})}(v_{i,t}, u_{i,t})$ contains movements to neighboring vertices in V_i . A busy patroller moves towards an incident or stays at the scene, moving back towards its beats afterward. After patrol actions, a dispatch action is selected from the dispatch action set $\mathcal{A}^{(\text{dispatch})}(\mathbf{v}'_t, \mathbf{w}'_t)$. Note, \mathbf{v}'_t and \mathbf{w}'_t refer to the updated \mathbf{v}_t and \mathbf{w}_t according to the patrol actions and the incident arrivals. The joint action space is

$$\mathcal{A}(\mathbf{v}_t, \mathbf{w}_t) = \mathcal{A}_1^{(\text{patrol})}(v_{1,t}, u_{1,t}) \times \cdots \times \mathcal{A}_N^{(\text{patrol})}(v_{N,t}, u_{N,t}) \times \mathcal{A}^{(\text{dispatch})}(\mathbf{v}_t', \mathbf{w}_t').$$

The patrol action space has exponential cardinality in N, and the dispatch action space has combinatorial cardinality.

3.3.3 Response-Based Reward & Objective.

The reward function is the negative sum of response times and a penalty for incidents removed from a capacitated queue:

$$R(t) = -\left(\sum_{j \text{ dispatched in iteration } t \text{ response}(i,j) + \sum_{j \text{ removed in iteration } t} \alpha \cdot t_{\text{idle}}(j)\right). \tag{3}$$

Penalty weight α is a hyper-parameter ($\alpha = 2$ in this work). Given $s_0 \in \mathcal{S}$,

$$\pi^{\star}(s_0) = \operatorname*{argmax}_{\pi \in \Pi} \mathbb{E}\left[\sum_{t \geq 0} \gamma^t R(t) \mid s_t \sim \mathbb{P}\left(s_{t-1}, \pi(s_{t-1})\right) \forall t > 0 \right].$$

3.3.4 Markov Game Decomposition.

Patrol and dispatch can be decomposed into an MG with N+1 agents defined by tuple:

$$\langle N+1, \mathcal{S}, \left\{\mathcal{S}_i^{(\mathrm{patrol})}\right\}_{i=1}^N \cup \mathcal{S}^{(\mathrm{dispatch})}, \left\{\mathcal{A}_i^{(\mathrm{patrol})}\right\}_{i=1}^N \cup \mathcal{A}^{(\mathrm{dispatch})}, \mathbb{P}, R, \gamma \rangle.$$

Patrol agent i corresponds to $\mathcal{A}_i^{(\text{patrol})}(v_{i,t}, u_{i,t})$ and the dispatch agent corresponds to $\mathcal{A}^{(\text{dispatch})}(\mathbf{v}_t', \mathbf{w}_t')$. Similar but distinct state spaces $\{\mathcal{S}_i^{(\text{patrol})}\}_{i=1}^N$ are defined so that each patrol agent observes its own perspective, swapping the location and busy status to the first index: $\mathbf{v}^{(i)} := [(v_i, u_i), \dots, (v_{i-1}, u_{i-1}), (v_1, u_1), (v_{i+1}, u_{i+1}), \dots, (v_N, u_N)]$. This yields $\mathcal{S}_i^{(\text{patrol})} = \{s = [\mathbf{v}^{(i)} \oplus \mathbf{w}]^T\}$. The dispatch agent observes joint state space $\mathcal{S}^{(\text{dispatch})} = \mathcal{S}$. Reward R(t) (3) is shared. The goal is to learn patrol policies $\pi_i^{(\text{patrol})}$ and dispatch policy $\pi^{(\text{dispatch})}$ to minimize the response time while avoiding incidents being removed from the queue.

4 Methodology

Parameter sharing in deep Q-learning is applied to learn patrol policies for each patroller (Section 4.1), and incidents are assigned to patrollers using a MIP and value function approximation (Section 4.2). These are combined to learn joint policies for patrol and dispatch (Section 4.3).

4.1 MARL with Parameter Sharing for Patrolling

The MG patrol policies (Section 3.3.4) are learned using MARL. Recall, in Section 3, the state spaces $\{S_i^{(\text{patrol})}\}_{i=1}^N$ are defined to contain the positions and statuses of all patrollers and incidents on the graph, while the action spaces $\{A_i^{(\text{patrol})}\}_{i=1}^N$ contain movements along the graph edges. Furthermore, all patrol agents share a reward R. Based upon prior MARL works indicating that similar agents benefit from parameter sharing (Gupta et al. 2017), this similarity in the state spaces, action spaces, and shared reward suggests that parameter sharing can be applied.

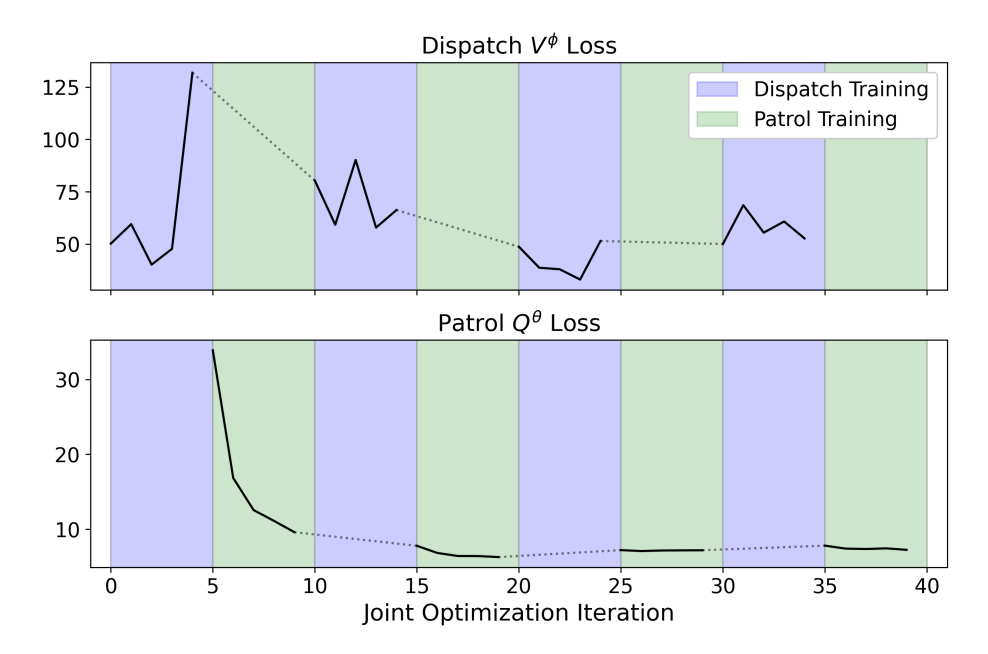


Figure 3: Loss of the dispatch and patrol value networks over the course of alternating joint optimization in the high call volume setting (Section 5.1).

Moreover, since the state spaces and action spaces are nearly identical, we employ an extreme version of parameter sharing in learning the patrol policies. That is, a single neural network Q^{θ} (parameterized by θ) learns a state-action value function for all agents. Our assumption is that the universal approximation power of a "large enough" neural network has the capacity to jointly learn all patrol policies, which is validated by the performance of the learned patrol policies in the experiments of Section 5. We find that DQNs of relatively few layers can learn these policies. Patrol policies thus select actions according to $\pi_i^{\theta}(s_i) = \underset{a}{\operatorname{argmax}} Q^{\theta}(s_i, a)$. Mini-batches of transitions $(s_{i,t}, a_{i,t}, r_t, s_{i,t+1})$ from each agent's perspective are collected via ϵ -greedy simulation to update Q^{θ} using LSVI updates.

4.2 Policy Iteration for Dispatching

A variation of the MIP action selection strategy outlined in Section 2.1.3 is employed for dispatch. Let $x_{ij} = 1$ if patroller i is assigned to incident j, otherwise let $x_{ij} = 0$. The first term of reward (3) can be computed given x_{ij} : $\sum_{i,j} t_{\text{response}}(i,j) \cdot x_{ij}$. Unlike Delarue et al. (2020), we cannot directly compute the entire reward, nor can we obtain the transition state deterministically due to incident queue "overflow" resulting from stochastic call arrival dynamics. This factor, and the difference in patroller positions due to the patrol policy, affects the state transition.

Given $V^{(\text{dispatch})}$ (or an approximation V^{ϕ}), the next-state value can be approximated. Define the value delta for patroller i as

$$\delta V_i^{(\text{dispatch})}(s) := \mathbb{E}\left[V^{(\text{dispatch})}(\text{patroller } i \text{ assigned}) - V^{(\text{dispatch})}(\text{patroller } i \text{ not assigned})\right] \tag{4}$$

and for incident j as

$$\delta V_j^{(\text{dispatch})}(s) := \mathbb{E}\left[V^{(\text{dispatch})}(\text{incident } j \text{ assigned}) - V^{(\text{dispatch})}(\text{incident } j \text{ not assigned})\right], \tag{5}$$

where the expectation is taken under the transition dynamics \mathbb{P} conditioned upon the policies for patrol and dispatch. These represent beginning in state s and considering the expected change in value for assigning patroller i to some idle incident, with no other assignments made. Given approximators $\delta V_i^{\phi_1}$ for $\delta V_i^{(\text{dispatch})}$

Table 1: Response time distribution characteristics (over 100 simulations of 5000 iterations) for the settings
of Section 5.1. Quantities in parenthesis are standard deviations. Notation $q = Q$ refers to the Q-quantile.

		High Cal	l Volume		Low Call Volume				
Policy	Avg. Response	Avg. Overflows	q = 0.75 Response	q = 0.95 Response	Avg. Response	Avg. Overflows	q = 0.75 Response	q = 0.95 Response	
Heuristic	10.0(5.90)	131 _{18.6}	14	21	7.07 _(4.81)	6.63 _(3.82)	9	16	
Patrol	$9.57_{(5.83)}$	$124_{20.4}$	13	20	$6.24_{(4.47)}$	$4.61_{(3.26)}$	8	15	
Dispatch	$8.13_{(5.43)}$	$77.5_{13.8}$	11	19	$7.16_{(4.10)}$	$53.5_{(10.0)}$	10	15	
Joint	$8.09_{(5.33)}$	$79.8_{14.6}$	11	18	$5.95_{(4.18)}$	$3.69_{(2.69)}$	8	14	

and $\delta V_j^{\phi_2}$ for $\delta V_j^{(\text{dispatch})},$ dispatch is formulated as the MIP:

$$\pi^{\phi}(s) = \underset{x}{\operatorname{argmin}} \sum_{i=1}^{N} \sum_{j=1}^{M} t_{\text{response}}(i, j) \cdot \left(x_{ij} - \delta V_i^{\phi_1}(s) - \delta V_j^{\phi_2}(s) \right)$$
s.t.
$$\sum_{j=1}^{M} x_{ij} \leq \mathbb{I}_{\{\text{patroller } i \text{ is free}\}} \quad \forall i \in \{1, \dots, N\}$$

$$\sum_{i=1}^{N} x_{ij} \leq \mathbb{I}_{\{\text{incident } j \text{ is idle}\}} \quad \forall j \in \{1, \dots, M\}$$

$$x_{ij} \in \{0, 1\} \quad \forall i \in \{1, \dots, N\}, j \in \{1, \dots, M\},$$

where $\mathbb{I}_{\{\text{event}\}}$ is an indicator for $\{\text{event}\}$. Notably, given $\delta V_i^{\phi_1}$ and $\delta V_j^{\phi_2}$, this can be computed deterministically given x_{ij} and the initial state s.

 $\delta V_i^{\phi_1}$ and $\delta V_j^{\phi_2}$ can be learned by first approximating $V^{(\text{dispatch})}$ using V^{ϕ} (Section 2.1.2). Using V^{ϕ} , mappings are generated from states to expectations (4)-(5). Approximators $\delta V_i^{\phi_1}$ and $\delta V_j^{\phi_2}$ are trained to map states to value deltas. We utilize a policy iteration scheme as in Delarue et al. (2020); we iterate between updating V^{ϕ} and updating $\delta V_i^{\phi_1}$ and $\delta V_j^{\phi_2}$ using V^{ϕ} . In practice, one network is learned for patrollers, δV^{ϕ_1} , and one network for incidents, δV^{ϕ_2} , which have output dimension equal to the number of patrollers and the size of the incident queue, respectively.

4.3 Joint Patrol & Dispatch Policy

The joint policy for patrol and dispatch combines the separate patrol and dispatch policies by optimizing their parameters alternatively. As described in Section 4.3.1, the parameters of the patrol policies are frozen when learning those of the dispatch policy, and vice versa. This alternating procedure is empirically found to converge to effective policies that outperform those optimized for patrol or dispatch alone (see Figure 3 and Section 5).

Given jointly-optimized policies for patrol and dispatch, the policy is deployed as follows: patroller i observes a state and moves according to π_i^{θ} . Incidents are sampled, and the dispatch agent matches patrollers to incidents according to π^{ϕ} . R(t) and joint state s_{t+1} are finally computed. The dispatcher observes the state as influenced by the patrol policy in the first phase, with reward and subsequent state observed by the patrollers being influenced by the dispatch policy. The assumption that the coordination of the patrollers and the dispatcher is enhanced by a joint optimization is validated by the improved performance of the jointly-optimized policies in our experiments.

4.3.1 Joint Policy Optimization

We alternatively optimize the parameters defining the patrol and dispatch policies. One phase involves Q-learning of the shared patroller Q^{θ} , while the other phase involves updates to the incident value networks

 V^{ϕ} , $\delta V_i^{\phi_1}$, and $\delta V_j^{\phi_2}$, repeating to convergence. For outer loop iterations, a number of inner loop updates are made to the dispatcher, followed by a number of inner loop updates to the patrollers. The steps of the $n_{\text{inner},\phi}$ inner loop updates to the dispatcher are:

- (1) collect transitions from on-policy simulation,
- (2) conduct $n_{\text{epoch},\phi}$ epochs of training for V^{ϕ} ,
- (3) generate "delta transitions" for each delta network using V^{ϕ} , and
- (4) conduct $n_{\text{epoch},\phi_1} = n_{\text{epoch},\phi_2}$ epochs of training on each network δV^{ϕ_1} and δV^{ϕ_2} .

The steps of the $n_{\text{inner},\theta}$ inner loop updates to the patrollers are:

- (1) collect transitions from ϵ -greedy on-policy simulation and
- (2) conduct $n_{\text{epoch},\theta}$ epochs of training for Q^{θ} .

This is repeated for $n_{\rm outer}$ outer loop iterations. We find that performance gains from learning dispatch policies are greater than patrol policies, so we begin optimization with a "warm-start" to the dispatch policy consisting of $n_{\rm warm}$ dispatch inner loop iterations. For the experiments of Section 5, all networks are multi-layer perceptrons (MLPs) using rectified linear unit (ReLU) activation. Dispatch inner loops train using $n_{\rm dispatch}$ number of transitions (per inner loop iteration), while patrol inner loops train using $n_{\rm patrol}$ transitions. All transitions are split into an 80%/20% train/validation split. The discount factor $\gamma=0.9$ in all settings.

5 Experiments

The experiments compare joint optimization of patrol and dispatch to policies optimized for patrolling or dispatch alone. In Section 5.1, the goal is to minimize the reward as defined in (3). Then, in Section 5.2, the reward is altered to demonstrate learning of more equitable policies. Finally, a real data example is outlined in Section 5.3 based on a region in the City of Atlanta. See Appendix A for a discussion of model selection in each experiment.

Baselines & Comparison. The three baselines include patrol-only optimization, dispatch-only optimization, and a fully heuristic policy. For policies without optimized patrol, patrollers move randomly in their assigned regions. For policies without optimized dispatch, dispatch follows a first come, first serve priority queue whereby incident class 2 precedes incident class 1, and the closest free patroller is sent to the scene. To compare policies, we evaluate incident response over $n_{\rm episode}$ episodes, each consisting of 5,000 iterations of on-policy simulation. The characteristics of the response time distributions are compared in addition to the number of incident queue overflows per episode.

5.1 Efficient Response Experiments

Simulated Settings. Consider two simulated settings on the same graph consisting of two 7×7 beats adjacent on one edge. Two categories of incident arrive with rates λ_1 and λ_2 , uniform distributions q_1 and q_2 , and average service times $\beta_1 = 1$ and $\beta_2 = 3$. The incident queue size is 3. In the **High Call Volume** setting, $\lambda_1 = 0.15$ and $\lambda_2 = 0.075$. In the **Low Call Volume** setting, $\lambda_1 = 0.075$ and $\lambda_2 = 0.05$.

Modeling & Optimization. Joint optimization is conducted using $n_{\text{outer}} = 4$ with $n_{\text{inner},\phi} = 5$ and $n_{\text{inner},\theta} = 5$ and beginning with $n_{\text{warm}} = 20$. Each dispatch inner loop trains for $n_{\text{epochs},\phi} = n_{\text{epochs},\phi_1} = n_{\text{epochs},\phi_2} = 25$ epochs each for V^{ϕ} , δV^{ϕ_1} , and δV^{ϕ_2} . This is conducted over $n_{\text{dispatch}} = 1,000$ simulated transitions per iteration with batch size 100 and learning rate 10^{-3} . Each patrol inner loop fixes $\epsilon = 1$ (fully random patrol) and trains for $n_{\text{epochs},\theta} = 1$ epochs for Q^{θ} , which is conducted over $n_{\text{patrol}} = 1.25$ million simulated transitions with batch size 50 and learning rate 10^{-5} . V^{ϕ} , δV^{ϕ_1} , and δV^{ϕ_2} are MLPs of 1 hidden layer with 128 nodes, while Q^{θ} is an MLP of 2 hidden layers with 512 nodes each. Validation

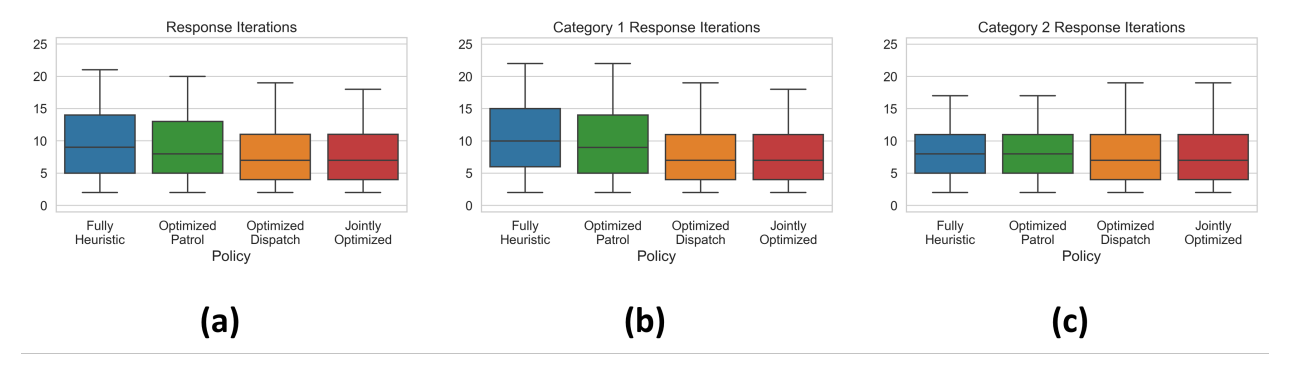


Figure 4: Response time distributions (a) for all incidents and (b)-(c) for each incident category in the high call volume setting of Section 5.1.

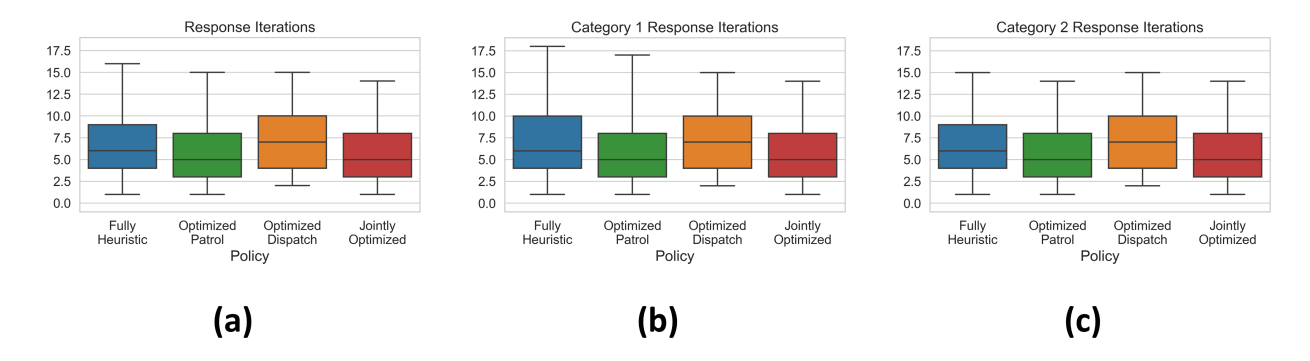


Figure 5: Response time distributions (a) for all incidents and (b)-(c) for each incident category in the low call volume setting of Section 5.1.

loss is visualized in Figure 3 for the high call volume setting. The dispatch dynamic is very noisy but still leads to an effective policy. The patrol-only optimization uses $n_{\text{inner},\theta} = 20$ updates to a patrol Q^{θ} network. The dispatch-only optimization uses $n_{\text{inner},\phi} = 50$ updates to dispatch networks. All other patrol- and dispatch-only optimization parameters are identical to those of the joint optimization.

Results. Response time distributions are generated using $n_{\rm episodes} = 100$. The high call volume experiment results are visualized in Table 1 and Figure 4. The jointly-optimized policy has the fastest response and loses few incidents. This and the dispatch-only optimized policy have similar response distributions. Response times are visualized by category in Figure 4(b)-(c); the jointly-optimized policy is best in category 1 with diminished performance in category 2. This could indicate that dispatch optimization yields policies that prefer incidents that take less time to manage (since $\beta_1 < \beta_2$), resulting in lower average response times. Table 1 and Figure 5 show the low call volume results. The jointly-optimized policy responds more quickly, and all policies lose a similarly small number of calls except for the dispatch-only optimized policy. In this case, the jointly-optimized policy has a similar response time to both categories.

5.2 Equity-based Reward

Simulated Setting. Figure 6(a) visualizes a graph of 119 nodes divided into two beats of 58 and 61 nodes. One incident category arrives with rate $\lambda = 0.2$ and has average service time $\beta = 3$. In Figure 6(b) and (c), it is revealed that the non-uniform incident distribution induces two *groups*. The smaller of these groups, **Group 1**, consists of 20 nodes and has incident probability ten times that of the larger group, **Group 2**, which consists of 99 nodes.

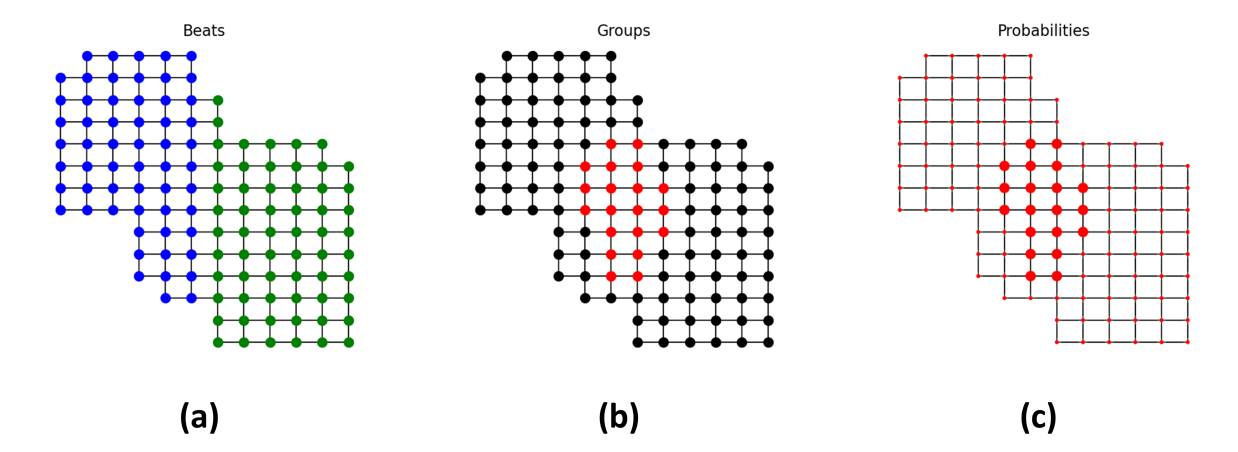


Figure 6: The graph setting of Section 5.2, which is divided into two beats in (a), as well as two *groups* in (b) and (c) which experience different rates of incident arrival.

Table 2: Response time distribution characteristics for Section 5.2. "Group Difference" refers to the difference in average response time between Group 2 and Group 1, and "Coverage Ratio" refers to the ratio of the number of iterations spent in Group 2 to Group 1.

	Group 1 (Small)				Group 2 (Large)				Overall		
Policy	Avg. Response	Avg. Overflows	q = 0.75 Response	q = 0.95 Response	Avg. Response	Avg. Overflows	q = 0.75 Response	q = 0.95 Response	Avg. Response	Group Difference	Coverage Ratio
Heuristic	9.07 _(5.10)	63.5(11.3)	12	19	12.0(5.66)	30.8(7.03)	16	22	10.0(5.47)	2.96	0.91
$\rho_{\text{large}} = 0.5$	$8.95_{(6.16)}$	$63.4_{(11.7)}$	11	21	$11.7_{(6.20)}$	$29.9_{(6.21)}$	15	24	$9.86_{(6.31)}$	2.75	1.40
$\rho_{\text{large}} = 1.0$	$8.11_{(5.46)}$	$49.3_{(10.8)}$	10	18	$11.8_{(7.50)}$	$38.8_{(8.37)}$	15	26	$9.28_{(6.42)}$	3.66	0.93

Fairness. An equity-based reward can be constructed to yield different penalties for each group:

$$\tilde{R}(t) = -\left(\sum_{j \text{ dispatched in iteration } t} \rho_j t_{\text{response}}(i, j) + \sum_{j \text{ removed in iteration } t} \rho_j \alpha \cdot t_{\text{idle}}(j)\right), \tag{6}$$

where ρ_j is the weight of the penalty incurred for the group in which j occurred. Additional metrics can be introduced to quantify fairness. The distribution of response times can be compared between the two groups; connecting to the independent notion of fairness (Barocas et al. 2017), response efficiency should be independent of the group. Similarly, a fair policy could be expected to cover each group for a fraction of iterations equal to the portion of the graph the group represents.

Modeling & Optimization. The networks V^{ϕ} , δV^{ϕ_1} , δV^{ϕ_2} , and Q^{θ} are structured and optimized exactly as in Section 5.1. Jointly-optimized policies trained using equitable reward (6) with different weights are compared. Specifically, the weight of the small group is fixed at $\rho_{\text{small}} = 1$, and the weight of the large group is $\rho_{\text{large}} \in \{0.5, 1.0\}$ representing weighted and unweighted policies, respectively.

Results. Response characteristics are compared using $n_{\text{episodes}} = 100$. The results are visualized in Table 2 and Figure 7. A discrepancy in average response time between the two groups is observed in all settings, but this is particularly pronounced in the "unfair" optimized setting ($\rho_{\text{large}} = 1.0$). This discrepancy is about an iteration smaller for the "fair" ($\rho_{\text{large}} = 0.5$), which is also an improvement over the heuristic. Moreover, the fair policy improves upon the overall response time of the heuristic policy while achieving a better balance in response. Coverage is compared using $n_{\text{episodes}} = 25$ simulations, and the results are compared in the final column of Table 2. The unfair and heuristic policies do a poor job of balancing coverage, while the fair policy does much better to cover the larger group. Appendix A outlines model selection for this section;

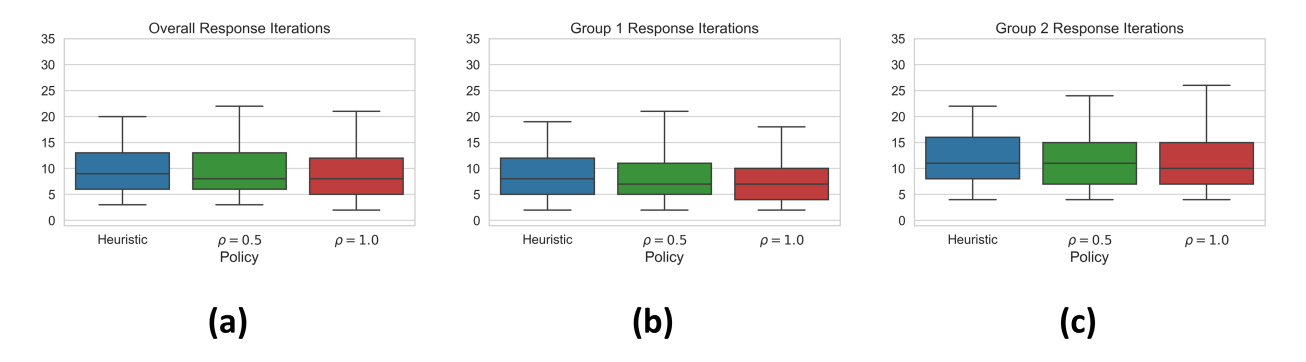


Figure 7: Response time distributions (a) for all groups and (b)-(c) for each group in the equity-based setting of Section 5.2.

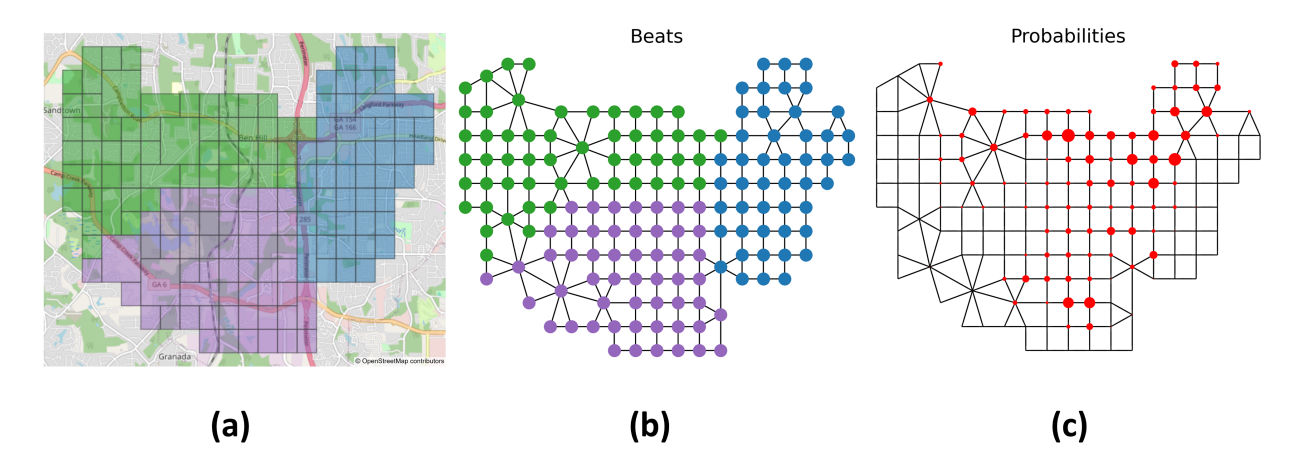


Figure 8: A region of Southwest Atlanta is partitioned into rectangular patches in (a), which are translated into a graph structure composed of 3 beats pictured in (b). In (c), the spatial distribution of incidents estimated from the calls-for-service data is visualized.

Table 3: Response time distribution characteristics for the setting based on the real data from the city of Atlanta described in Section 5.3.

Policy	Avg.	Avg.	q = 0.75	q = 0.95
	Response	Overflows	Response	Response
Real Heuristic Patrol Dispatch Joint	$11.7_{(5.62)} \\ 11.4_{(5.73)} \\ 11.3_{(5.74)} \\ 9.50_{(6.91)} \\ 9.39_{(6.66)}$	$110_{17.8} \\ 104_{20.5} \\ 107_{18.5} \\ 99_{19.2} \\ 92_{17.2}$	16 15 15 12 12	22 21 21 22 22

Figure 11 reveals that the unfair ($\rho_{\text{large}} = 1.0$) policy has a large discrepancy in average response throughout training, which is not the case for the fair policy. Both policies can experience similar coverage ratios, but this can come at a cost to a balanced or effective response.

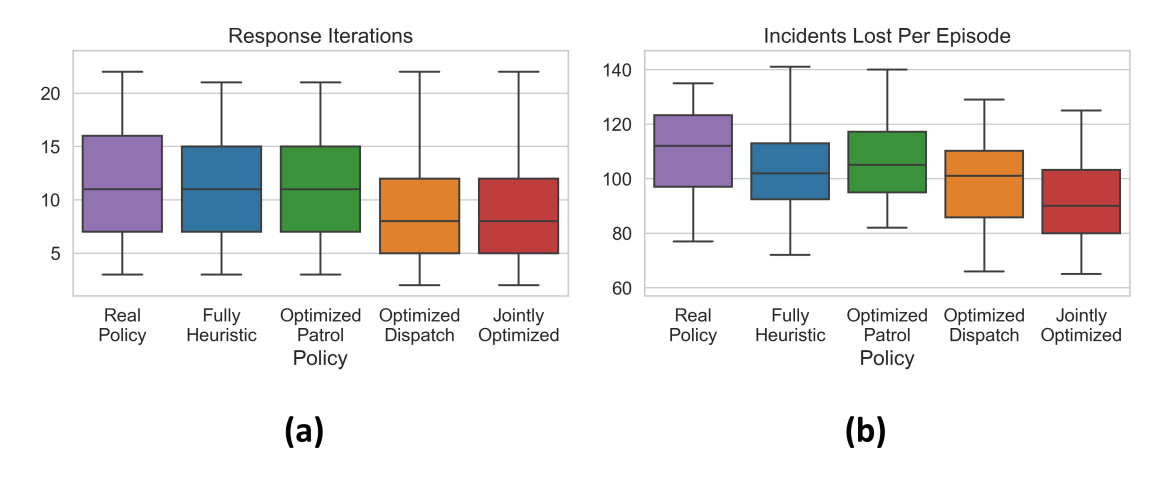


Figure 9: In (a), response time distributions are visualized for the application to the setting based on the city of Atlanta described in Section 5.3. Similarly, (b) displays the distributions of incidents lost per episode.

5.3 Southwest Atlanta Beats

Environment Setting. The graph environment in this experiment is based upon a 3-beat region in Southwest Atlanta, which is discretized into 154 rectangular partitions representing nodes on the spatial graph. See Figure 8(a); the patches are selected based on APD patroller trajectory data discretized into 1-minute intervals. The patches are constructed such that observed trajectories take approximately 1 iteration (i.e., 1 minute) to travel between adjacent patches. In Figure 8(b), the resultant graph is shown, which is divided into three beats with one patroller per beat. Finally, as shown in Figure 8(c), incidents are spatially distributed according to a distribution estimated given the \sim 90k APD calls-for-service from January 1, 2009 to January 8, 2012. The temporal intensity $\lambda = 0.25$ per iteration and service time $\beta = 5$ iterations.

Real Policy. An additional baseline is developed for this setting based on limited APD patroller trajectory data. That is, divided into 1-minute time intervals, APD patroller trajectories over a 2-day interval are tracked along the graph structure. Transitions to adjacent nodes are counted, and the resultant policy ranks potential actions according to the frequency with which each edge was traversed in the real trajectory data. This is denoted the "Real Policy," and can reflect some information about how the police patrol in practice. This policy also uses a first come, first serve queue for dispatch.

Modeling & Optimization. Joint optimization is conducted using $n_{\text{outer}} = 8$ with $n_{\text{inner},\phi} = 10$ and $n_{\text{inner},\theta} = 5$ with 0 warm-start iterations. The dispatch networks are trained using $n_{\text{dispatch}} = 10,000$ simulated transitions per inner loop iteration, while all other optimization parameters for patrol and dispatch are identical to those described in Section 5.1. For comparison, patrol-only optimization uses $n_{\text{inner},\phi} = 40$ and dispatch-only optimization uses $n_{\text{inner},\phi} = 80$. As before, the patrol- and dispatch-only optimization parameters are identical to those of the joint optimization.

Results. In Figure 9 and Table 3, the response time distributions for each policy are represented over $n_{\rm episodes} = 100$ episodes. While the jointly-optimized policy has the fastest response on average, the overall response time distribution characteristics are similar to those of the dispatch-only optimized policy. However, as shown in Figure 9(b), the jointly-optimized policy loses substantially fewer incidents per episode than the other policies, indicating that it is the most effective overall policy. Moreover, the jointly-optimized policy leads to faster response and fewer incidents lost than the realistic policy. This suggests that (joint) policy optimization can lead to substantial improvements when applied to real-world environments.

6 Conclusion

We have outlined a novel procedure for the joint optimization policies for patrol and dispatch using MARL. The patrol policies are learned using deep Q-learning with parameter sharing, and the dispatch policies are learned using a policy iteration scheme based on MIP action selection. These policies are combined in a joint optimization procedure that follows a coordinate-descent-style scheme, iteratively updating patrol policies given fixed dispatch policy and vice versa. Within this framework, we extend previous works addressing combinatorial action selection in RL via an MIP approach, where our novel procedure facilitates action selection in settings with stochastic state transitions. We comprehensively demonstrate that policies learned using this joint optimization approach outperform those optimized for patrol or dispatch alone, in addition to heuristics such as random patrol and priority-queue-based dispatch.

The experiments of Section 5.1 reveal that the joint optimization procedure is robust to settings with a range of incident arrival dynamics. In the high call volume setting, the jointly-optimized policy performs similarly to the dispatch-only optimized policy. In the low call volume setting, the jointly-optimized policy performs similarly to the patrol-only optimized policy. The jointly-optimized policy is the only policy to perform effectively in both settings. In Section 5.2, a modified reward is used to obtain more fair policies than those trained "greedily". The results reveal that our procedure is flexible to the reward definition and can generate policies that yield more balanced responses and coverage across groups. While there is still much room for improvement according to the equity-based metrics, this represents a promising direction for further research within the framework of joint policy optimization. Finally, Section 5.3 suggests that the outlined method applies to real-world scenarios by applying joint policy optimization to a setting based on Southwest Atlanta. A comparison to a realistic policy based on real patroller trajectory data reveals significant improvements in response time distribution characteristics due to policy optimization; particularly, jointly-optimized policies for patrol and dispatch are most effective.

Future work can incorporate additional incident-level information in the decision-making process. For instance, the experiment of Section 5.2 indicates that the encoding of group attributes in the reward can lead to a more equitable response. As with prior works considering fairness in police patrol and dispatch, incidents can also include information regarding socioeconomic and racial status, going beyond the geographic location-based fairness demonstrated in this work. Algorithmically, future research can also focus on the incorporation of fairness into the learning procedure itself, drawing inspiration from prior work on fairness in learning for contextual bandits (Joseph et al. 2016) and RL (Jabbari et al. 2017). Such studies require that certain equity constraints are satisfied throughout the learning process, which could be relevant to online learning of policies for patrol and dispatch.

Acknowledgement

This work is partially supported by an NSF CAREER CCF-1650913, NSF DMS-2134037, CMMI-2015787, CMMI-2112533, DMS-1938106, DMS-1830210, and the Coca-Cola Foundation.

References

Almeida A, Ramalho G, Santana H, Tedesco P, Menezes T, Corruble V, Chevaleyre Y (2004) Recent advances on multi-agent patrolling. Advances in Artificial Intelligence—SBIA 2004: 17th Brazilian Symposium on Artificial Intelligence, Sao Luis, Maranhao, Brazil, September 29-Ocotber 1, 2004. Proceedings 17, 474–483 (Springer).

Atlanta Police Department (2023) APD Zones. Accessed Mar. 27, 2023 [Online], URL https://www.atlantapd.org/community/apd-zones.

Barocas S, Hardt M, Narayanan A (2017) Fairness in machine learning. Nips tutorial 1:2017.

Bertsekas D (2019) Reinforcement learning and optimal control (Athena Scientific).

Bradtke SJ, Barto AG (1996) Linear least-squares algorithms for temporal difference learning. *Machine learning* 22(1-3):33–57.

Charalambous Ρ (2023)'vicious cycle': Inside the police recruiting rise. ABCNewsURL with resignations the https://abcnews.go.com/US/ police-departments-face-vicious-cycle-challenges-retaining-recruiting/story?id=98363458.

- Chen D, Li Z, Wang Y, Jiang L, Wang Y (2021) Deep multi-agent reinforcement learning for highway on-ramp merging in mixed traffic. arXiv preprint arXiv:2105.05701.
- Chevaleyre Y (2004) Theoretical analysis of the multi-agent patrolling problem. *Proceedings. IEEE/WIC/ACM International Conference on Intelligent Agent Technology, 2004.(IAT 2004).*, 302–308 (IEEE).
- Christianos F, Papoudakis G, Rahman MA, Albrecht SV (2021) Scaling multi-agent reinforcement learning with selective parameter sharing. *International Conference on Machine Learning*, 1989–1998 (PMLR).
- Chu X, Ye H (2017) Parameter sharing deep deterministic policy gradient for cooperative multi-agent reinforcement learning. arXiv preprint arXiv:1710.00336 .
- Delarue A, Anderson R, Tjandraatmadja C (2020) Reinforcement learning with combinatorial actions: An application to vehicle routing. Advances in Neural Information Processing Systems 33:609–620.
- Dickson ES, Gordon SC, Huber GA (2022) Identifying legitimacy: Experimental evidence on compliance with authority. *Science Advances* 8(7):eabj7377.
- Dunnett S, Leigh J, Jackson L (2019) Optimising police dispatch for incident response in real time. *Journal of the Operational Research Society* 70(2):269–279.
- Eckhouse L, Lum K, Conti-Cook C, Ciccolini J (2019) Layers of bias: A unified approach for understanding problems with risk assessment. *Criminal Justice and Behavior* 46(2):185–209.
- Farinelli A, Iocchi L, Nardi D (2017) Distributed on-line dynamic task assignment for multi-robot patrolling. Autonomous Robots 41:1321–1345.
- Green L (1984) A multiple dispatch queueing model of police patrol operations. Management science 30(6):653-664.
- Guedes R, Furtado V, Pequeno T (2015) Multi-objective evolutionary algorithms and multiagent models for optimizing police dispatch. 2015 IEEE International Conference on Intelligence and Security Informatics (ISI), 37–42 (IEEE).
- Gupta JK, Egorov M, Kochenderfer M (2017) Cooperative multi-agent control using deep reinforcement learning.

 Autonomous Agents and Multiagent Systems: AAMAS 2017 Workshops, Best Papers, São Paulo, Brazil, May 8-12, 2017, Revised Selected Papers 16, 66-83 (Springer).
- Hermann P (2023) D.c. police staffing reaches half-century low as homicides rise. The Washington Post URL https://www.washingtonpost.com/dc-md-va/2023/04/15/dc-police-staffing-crime/.
- Jabbari S, Joseph M, Kearns M, Morgenstern J, Roth A (2017) Fairness in reinforcement learning. *International conference on machine learning*, 1617–1626 (PMLR).
- Jana M, Vachhani L, Sinha A (2022) A deep reinforcement learning approach for multi-agent mobile robot patrolling. International Journal of Intelligent Robotics and Applications 6(4):724–745.
- Joseph M, Kearns M, Morgenstern JH, Roth A (2016) Fairness in learning: Classic and contextual bandits. Advances in neural information processing systems 29.
- Kaste M (2023) Why data from 15 cities shows police response times are taking longer (accessed April 30, 2024). Https://www.npr.org/2023/01/17/1149455678/why-data-from-15-cities-show-police-response-times-are-taking-longer.
- Liberatore F, Camacho-Collados M, Quijano-Sánchez L (2022) Equity in the police districting problem: balancing territorial and racial fairness in patrolling operations. *Journal of Quantitative Criminology* 38(3):1–25.
- Liberatore F, Camacho-Collados M, Quijano-Sánchez L (2023) Towards social fairness in smart policing: Leveraging territorial, racial, and workload fairness in the police districting problem. *Socio-Economic Planning Sciences* 87:101556.
- Littman ML (1994) Markov games as a framework for multi-agent reinforcement learning. *Machine learning proceedings* 1994, 157–163 (Elsevier).
- Machado A, Ramalho G, Zucker JD, Drogoul A (2003) Multi-agent patrolling: An empirical analysis of alternative architectures. *Multi-Agent-Based Simulation II: Third International Workshop, MABS 2002 Bologna, Italy, July 15–16, 2002 Revised Papers*, 155–170 (Springer).
- Mnih V, Kavukcuoglu K, Silver D, Rusu AA, Veness J, Bellemare MG, Graves A, Riedmiller M, Fidjeland AK, Ostrovski G, et al. (2015) Human-level control through deep reinforcement learning. *nature* 518(7540):529–533.
- Notre Dame Police Department (2024) Equity in policing. URL https://police.nd.edu/equity-in-policing/.
- Parker Police Department (2024) Equitable and fair policing practices. URL http://parkerpd.org/2041/ Equitable-and-Fair-Policing.
- Portugal D, Couceiro MS, Rocha RP (2013) Applying bayesian learning to multi-robot patrol. 2013 IEEE International Symposium on Safety, Security, and Rescue Robotics (SSRR), 1–6 (IEEE).

- Portugal D, Rocha R (2010) Msp algorithm: multi-robot patrolling based on territory allocation using balanced graph partitioning. *Proceedings of the 2010 ACM symposium on applied computing*, 1271–1276.
- Santana H, Ramalho G, Corruble V, Ratitch B (2004) Multi-agent patrolling with reinforcement learning. Autonomous Agents and Multiagent Systems, International Joint Conference on, volume 4, 1122–1129 (IEEE Computer Society).
- Stanford DA, Taylor P, Ziedins I (2014) Waiting time distributions in the accumulating priority queue. Queueing Systems 77:297–330.
- Sutton RS, Barto AG (2018) Reinforcement learning: An introduction (MIT press).
- Tampuu A, Matiisen T, Kodelja D, Kuzovkin I, Korjus K, Aru J, Aru J, Vicente R (2017) Multiagent cooperation and competition with deep reinforcement learning. *PloS one* 12(4):e0172395.
- Tan M (1993) Multi-agent reinforcement learning: Independent vs. cooperative agents. *Proceedings of the tenth international conference on machine learning*, 330–337.
- Terry JK, Grammel N, Son S, Black B (2020) Parameter sharing for heterogeneous agents in multi-agent reinforcement learning. arXiv e-prints arXiv-2005.
- The Associated Press (2023) The u.s. is experiencing a police hiring crisis. NBC News URL https://www.nbcnews.com/news/us-news/us-experiencing-police-hiring-crisis-rcna103600.
- Waldschmidt R (2018) Perspective: Fairness in law enforcement. URL https://leb.fbi.gov/articles/perspective/perspective-fairness-in-law-enforcement.
- Walker J (2023) The importance of equity in policing our community. URL https://today.uconn.edu/2023/04/the-importance-of-equity-in-policing-our-community/#.
- Watkins CJCH (1989) Learning from delayed rewards. Ph.D. thesis, University of Cambridge.
- Wheeler AP (2020) Allocating police resources while limiting racial inequality. Justice quarterly 37(5):842-868.
- Yu J, Vincent JA, Schwager M (2022) Dinno: Distributed neural network optimization for multi-robot collaborative learning. *IEEE Robotics and Automation Letters* 7(2):1896–1903.
- Zhang H, Jackson L, Tako A, Liu J (2016) A simulation of a police patrol service system with multi-grade time-varying incident arrivals. *Proceedings of the Operational Research Society Simulation Workshop 2016*.

A Model Selection

A.1 Model Selection in Section 5.1

In the experiments of Section 5.1, the desired policy is that which responds to incidents most efficiently. As such, the average response time is tracked over $n_{\text{episodes}} = 100$ of on-policy validation simulation over the course of optimization for each of the three optimized policies in each setting. This is depicted for the high call volume setting in Figure 10(a), which demonstrates that the policies corresponding to the minimum average response time are the jointly-optimized policy after iteration 22, the patrol-only optimized policy after iteration 9. Similarly, in the low call volume setting depicted in Figure 10(b), the selected policies are the jointly-optimized policy after iteration 35, the patrol-only optimized policy after iteration 19, and the dispatch-only optimized policy after iteration 7.

A.2 Model Selection in Section 5.2

In the experiment of Section 5.2, the goal is to find a policy that minimizes the difference in average response time between the two groups while balancing coverage. The characteristics of the "unfair" ($\rho_{\text{large}} = 1.0$) policy over the course of training are depicted in Figure 11(a), where coverage is computed using $n_{\text{episodes}} = 25$ on-policy validation simulations in each iteration, and response time characteristics are computed over $n_{\text{episodes}} = 100$ simulations (the same is true of the "fair" policy in Figure 11(b)). With the goal of this section in mind, the unfairly selected policy corresponds to iteration 66, which has a minimal average difference in response time and comparable coverage to the heuristic policy. The fair policy is chosen similarly - the goal is to balance fair response and fair coverage while still yielding an "effective policy". With this in mind, while iteration 23 corresponds to the most balanced average response in the top panel of Figure 11(b), the policy is not "effective" since there is a very large number of incident queue overflows (bottom panel). Therefore, the fair ($\rho_{\text{large}} = 0.5$) policy used in Section 5.2 corresponds to the optimized policy after iteration 36, which improves upon the balancing of average response time (second panel) while maintaining few overflows of the incident queue (bottom panel) and yielding a better coverage ratio (top panel).

A.3 Model Selection in Section 5.3

Just as in Section 5.1 and Appendix A.1, in the experiment of Section 5.3, the policy is selected to minimize the average response time. Therefore, this metric is tracked over $n_{\text{episodes}} = 100$ on-policy simulated episodes throughout the optimization of each policy. This is visualized in Figure 12, indicating that the optimal policies are those after iteration 110 for the jointly-optimized policy, after iteration 33 for the patrol-only optimized policy, and after iteration 77 for the dispatch-only optimized policy.

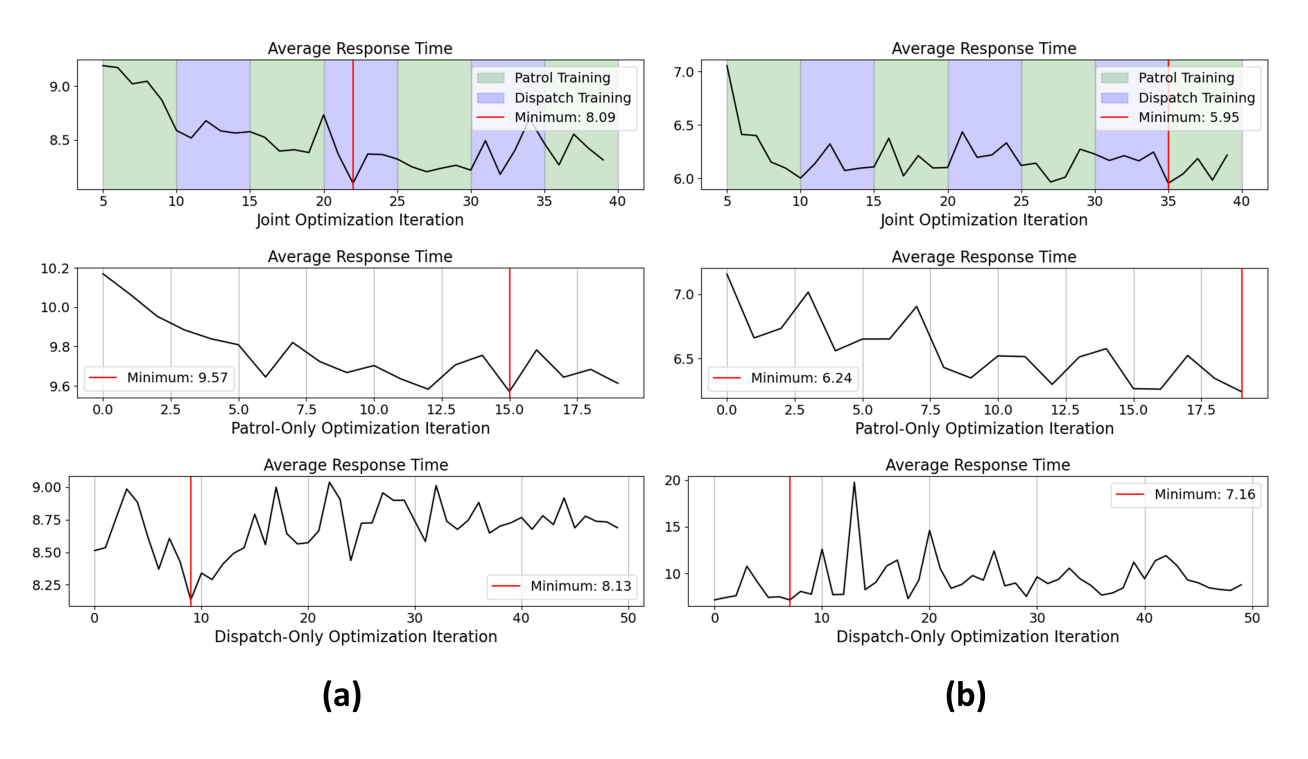


Figure 10: In the experiments of Section 5.1, the goal is to generate a policy that efficiently responds to incidents. The average response time is tracked over the course of training using $n_{\rm episodes} = 100$ validation simulations per iteration, and the policy with the lowest average response time is selected.

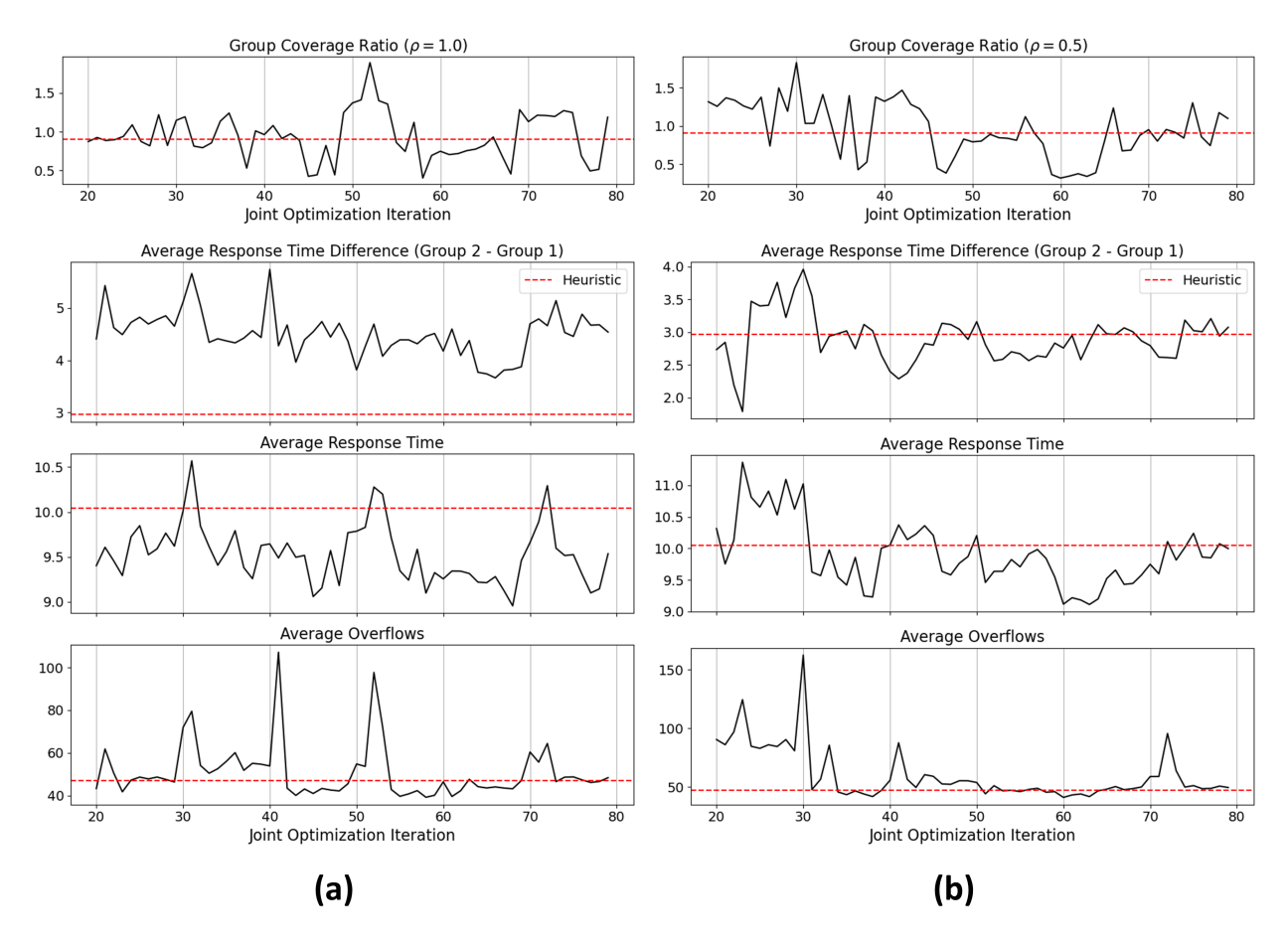


Figure 11: In the experiments of Section 5.2, the goal is to balance response time and coverage across groups. These metrics are tracked through training for the "unfair" policy in (a) and the "fair" policy in (b). In each case, the optimized networks are selected to balance these two metrics (first and second rows), subject to constraints on the effectiveness of the policies (third and fourth rows).

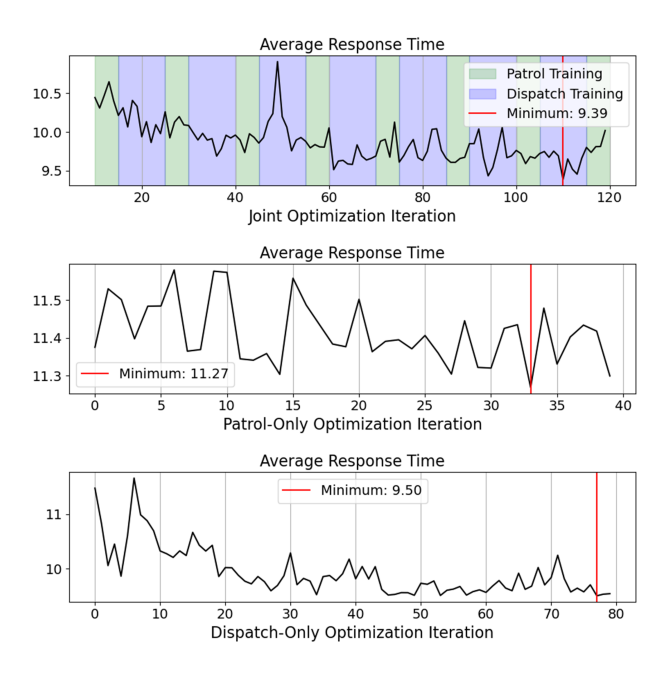


Figure 12: As with the first set of experiments, in the experiment of Section 5.3, the average response time is computed using $n_{\rm episodes}=100$ validation simulations per iteration of training. The fastest-average-response policy is selected, subject to a constraint that the average number of overflows is less than 1.25 times that of the heuristic policy.